

## Diimide-Mediated Hydrogenation of Nitrile Butadiene Rubber

(Penghidrogenan Pengantaraan Diimida bagi Getah Nitril Butadiena)

AMIRA SHAFIQA SALLEH HUDDIN<sup>1</sup>, YI-FAN GOH<sup>2</sup>, NAHARULLAH JAMALUDDIN<sup>3</sup> & SITI FAIRUS MOHD YUSOFF<sup>1,4,\*</sup>

<sup>1</sup>*Department of Chemical Sciences, Faculty of Science and Technology, Universiti Kebangsaan Malaysia, 43600 UKM Bangi, Selangor, Malaysia*

<sup>2</sup>*Asia Innovation Centre (AIC), Synthomer Sdn Bhd, Kawasan Perindustrian i-Park, Bandar Indahpura, 81000 Kulai, Johor, Malaysia*

<sup>3</sup>*Department of Chemistry, Faculty of Science, Universiti Teknologi Malaysia, 81310 Skudai, Johor, Malaysia*

<sup>4</sup>*Polymer Research Centre (PORCE), Faculty of Science and Technology, Universiti Kebangsaan Malaysia, 43600 UKM Bangi, Selangor, Malaysia*

Received: 19 January 2024/Accepted: 19 July 2024

### ABSTRACT

The hydrogenation of nitrile butadiene rubber (NBR) has shown great potential for improving its physical, thermal, mechanical, and chemical stability. Hydrogenation process of NBR in this work involved the utilization of diimide produced from the interaction between hydrazine hydrate ( $N_2H_4$ ) and hydrogen peroxide ( $H_2O_2$ ), with the addition of boric acid as a promoter. Attenuated total reflectance Fourier transform infrared (ATR-FTIR), differential scanning calorimetry (DSC), thermogravimetric analysis (TGA), and X-ray diffraction (XRD) were used to evaluate the degree of hydrogenation, glass transition, thermal stability, and rubber crystallinity, respectively. The highest hydrogenation degree was 99%, which resulted in a 57% gel content. Upon hydrogenation, both the glass transition temperature ( $T_g$ ) and decomposition temperature ( $T_d$ ) increased. The hydrogenated rubber samples generally showed an amorphous state, except for the 99% hydrogenated sample, which displayed a semi-crystalline state. However, using diimide for direct hydrogenation yields a side reaction from the free radicals in the system, which leads to gel formation. Optimization was accomplished by employing the response surface methodology (RSM), which entailed manipulating parameters such as the total solid content (TSC) of NBR, reaction time, and the mole ratio of  $H_2O_2$  to  $N_2H_4$ , to reduce the percentage of gel content. The RSM analysis identified the optimum reaction conditions as a 1:1 mole ratio of  $H_2O_2$ :  $N_2H_4$  and 25% TSC, with a reaction time of 8 h, which yielded 32% gel content percentage, where a mole ratio of  $H_2O_2$  to  $N_2H_4$  and reaction time indicated a synergistic effect, whereas TSC denoted an antagonistic effect.

Keywords: Diimide; gel content; hydrogenation; nitrile butadiene rubber; response surface methodology

### ABSTRAK

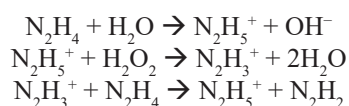
Penghidrogenan getah nitril butadiena (NBR) telah menunjukkan potensi besar untuk meningkatkan kestabilan fizikal, haba, mekanik dan kimianya. Proses penghidrogenan NBR dalam kajian ini melibatkan penggunaan diimida yang dihasilkan daripada interaksi antara hidrazin hidrat ( $N_2H_4$ ) dan hidrogen peroksida ( $H_2O_2$ ), dengan penambahan asid borik sebagai promoter. Spektroskopi jumlah pantulan dilemahkan- inframerah transformasi Fourier (ATR-FTIR), kalorimetri imbasan pembezaan (DSC), analisis termogravimetrik (TGA) dan pembelauan sinar-X (XRD), digunakan untuk menilai darjah penghidrogenan, peralihan kaca, kestabilan terma dan sifat kehabluran getah. Darjah penghidrogenan tertinggi yang dicapai ialah 99%, menghasilkan kandungan gel sebanyak 57%. Selepas penghidrogenan, kedua-dua suhu peralihan kaca ( $T_g$ ) dan suhu penguraian ( $T_d$ ) meningkat. Sampel getah terhidrogenasi menunjukkan keadaan amorfus, manakala sampel getah dengan 99% peratusan penghidrogenan, memaparkan keadaan separa kristal. Walau bagaimanapun, diimida menghasilkan tindak balas sampingan daripada radikal bebas dalam sistem, yang membawa kepada pembentukan gel. Pengoptimuman dicapai dengan menggunakan kaedah rangsangan permukaan (RSM), dengan menggunakan parameter yang dimanipulasi, iaitu jumlah kandungan pepejal (TSC) NBR, masa tindak balas dan nisbah mol  $H_2O_2$  kepada  $N_2H_4$ , untuk mengurangkan peratusan kandungan gel. Analisis RSM mengenal pasti keadaan tindak balas optimum sebagai nisbah mol 1:1  $H_2O_2$ : $N_2H_4$  dan 25% TSC, dengan masa tindak balas selama 8 jam yang menghasilkan 32% kandungan gel dengan nisbah molar  $H_2O_2$  kepada  $N_2H_4$  menunjukkan kesan sinergistik, sementara TSC dan masa tindak balas menunjukkan kesan antagonis.

Kata kunci: Diimida; getah nitril butadiena; kandungan gel; kaedah rangsangan permukaan; penghidrogenan

## INTRODUCTION

Hydrogenation of nitrile butadiene rubber (NBR) (Figure 1) has attracted considerable attention due to its capability to improve physical, mechanical, thermal, and chemical resistance properties. These enhancements offer significant advantages across a wide range of application in rubber industries (Zhang et al. 2020). The traditional methods of hydrogenating NBR faced major challenges, such as the expensive equipment required for handling high-pressure hydrogen gas, the utilization of complex metal catalytic systems, complicated procedures, and the use of organic solvents that posed a potential threat to the environment (Luo et al. 2019). Furthermore, the traditional approach commonly utilized homogeneous noble metal catalysts to attain a significant degree of hydrogenation. However, these catalysts frequently persisted in the hydrogenated product, resulting in high cost of separation and product deterioration. In addition, the products obtained through traditional procedure were generally in the form of bulk rubber, which limit their practical usage (Lin 2005; Luo et al. 2019).

Subsequently, researchers attempted to develop a technique that would effectively tackle the difficulties faced in the traditional methodology. The approached diimide ( $N_2H_2$ ) hydrogenation method was able to convert NBR into hydrogenated NBR (HNBR) without the need for high-pressure hydrogen gas, metal catalysts, organic solvents, or complicated procedures. This discovery utilized a redox system that involved the combination of hydrazine hydrate ( $N_2H_4$ ) and hydrogen peroxide ( $H_2O_2$ ), with boric acid as the promoter. The hydrogenation was carried out using rubber in its latex form and conducted at temperature below 100 °C to achieve selective hydrogenation and avoid undesired side reactions (Wang et al. 2020). The redox reaction between  $N_2H_4$  and  $H_2O_2$  generated  $N_2H_2$  as shown in Scheme 1, is crucial to produce hydrogen atoms in hydrogenation reaction.



SCHEME 1. Redox reaction between  $N_2H_4$  and  $H_2O_2$  (Yusof et al. 2018)

Figure 2 depicts the hydrogenation process of liquid NBR using diimide to form HNBR. It was discovered that the rubber generated from the hydrogenation of NBR using diimide were solidified due to the high gel content (Lin 2005). Hence, the diimide-mediated hydrogenation approach has constrained viability in the marketplace. Also, an increase in the degree of hydrogenation leads to a higher gel content. Gel formation is often considered an undesirable outcome in hydrogenation processes, as it can adversely affect the properties of the rubber (Liu et al.

2022). Rubber with a high gel content is more difficult to be processed in the manufacturing line. The presence of gel can cause uneven distribution within the rubber compound, which negatively impacts the uniformity and quality of the finished product. This can pose significant challenges in applications, where the rubber surface must have a high level of smoothness or strong adhesion to other materials, such as in gaskets or coatings. Gel formation often modifies the mechanical properties of rubber, leading to increased stiffness and reduced flexibility. Excessive gel content in car tyres or seals can cause decreased durability and increased vulnerability to cracking or failure in dynamic circumstances (Ngudsuntear, Limtrakul & Arayapranee 2022). The formation of gel is primarily attributed to the presence of crosslinks in the polymer structure. These crosslinks resulted from the reactions between diimide and multiple unsaturated sites in the polymer, as well as from the multiple side reactions that occurred in the system. As hydrogenation progressed, these crosslinks increased, which resulting in a higher gel content (Zhou, Bai & Wang 2004).

The raw material of NBR naturally contains some gel composition, and further modification processes enhance the polymer's crosslinking, resulted to gel content increase. Additionally, the  $H_2O_2$  used in the hydrogenation process comprises of oxygen-oxygen bond or peroxide bond, which is exceedingly weak and unstable, making it prone to the formation of side-reactions (Yusof et al. 2018). Furthermore, additional reactions were likely to have occurred alongside the hydrogenation phenomenon, based on the reactivity of diimide. One of the reactions was the interaction between diimide and  $H_2O_2$ , leading to the production of nitrogen and water (Lin 2005; Puspitasari, Falaah & Zanki 2019). This reaction has most likely occurred in the interphase because the  $H_2O_2$  is found in the water phase. Another reaction that likely to have taken place in the rubber phase is the interaction between two diimide molecules, resulting in the formation of one hydrazine molecule and the release of one nitrogen molecule (Nguyen Duy et al. 2021).

The rise in gel content had a positive correlation with an elevated degree of hydrogenation. The primary factor influencing the gel formation seems to be the quantity of  $H_2O_2$ . For example, epoxidized natural rubber (ENR) with 50% of an initial epoxide group concentration yielded 27.54% gel content. However, hydrogenation of ENR at around 89.19% seems to increase its gel content up to 63.64% (Ngudsuntear, Limtrakul & Arayapranee 2022a). Furthermore, the incorporation of antioxidants does not control the gel formation in the hydrogenation process of NBR using diimide (Lin 2005). On the other hand, the gel content is significantly influenced by the parameters utilized in the hydrogenation process (Yusof et al. 2018; Zhou, Bai & Wang 2004).

Our study focuses on a thorough examination of the hydrogenation process of NBR latex using the  $N_2H_4/H_2O_2$  system. The schematic representation of the interaction between organic and aqueous phases in the hydrogenation process is shown in Figure 3. This process leads to the formation of HNBR with mild reaction conditions. Also, this study evaluates the chemical, thermal, and mechanical stability of HNBR compared to the performance of controlled NBR. In addition, response surface methodology (RSM) was employed to determine the most optimum process parameters that minimize the amount of gel content, which is a crucial aspect in the production of rubber. The objective of our research was to acquire a thorough comprehension of the hydrogenation process, including any side reactions that may occur during the process. The results of this

study could improve the quality and effectiveness of the hydrogenation process for NBR latex, which has a huge impact on the rubber industries due to HNBR's good physical, thermal, chemical, and mechanical properties.

## EXPERIMENTAL DETAILS

### REAGENTS AND SOLUTIONS

The NBR latex with 45% total solid content (TSC) and Wingstay L antioxidants (consisted of poly(dicyclopentadiene-co-p-cresol)) were supplied by Synthomer Sdn. Bhd.  $N_2H_4$  (80% purity) and boric acid were purchased from Sigma Aldrich and J. K. Baker Co., respectively. Aqueous  $H_2O_2$  (35% purity), sodium dodecyl sulfate (SDS) (~99%), and methyl ethyl ketone were purchased from Bendosen.

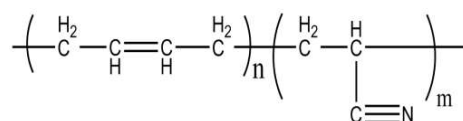


FIGURE 1. Chemical Structure of NBR

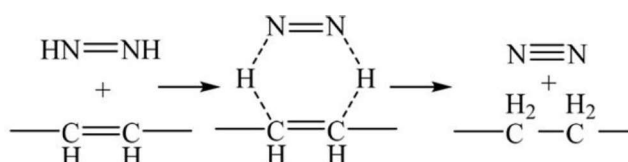


FIGURE 2. Overall chemical reaction of hydrogenation of NBR

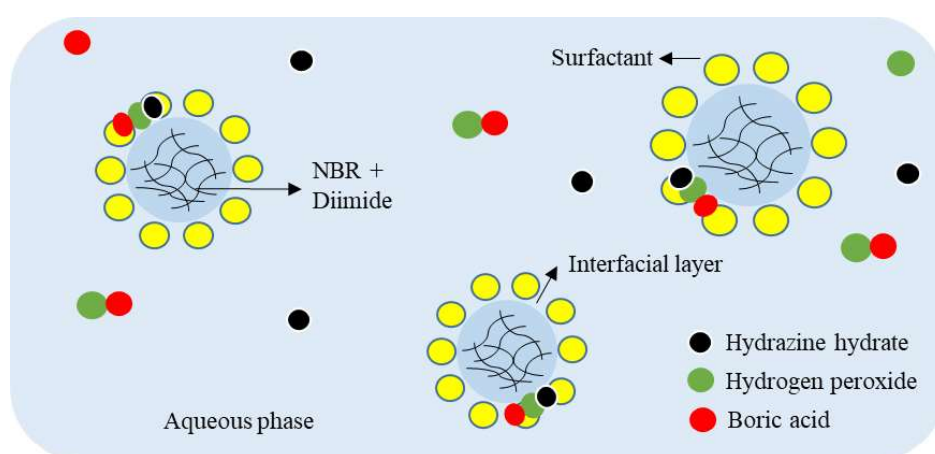


FIGURE 3. Schematic diagram of hydrogenation interaction system

SYNTHESIS OF HYDROGENATED NITRILE  
BUTADIENE RUBBER (HNBR)

HNBR was synthesized using the reflux method in a one-way process. First, NBR latex (100.0 g) was stirred in a 1000 mL round bottom flask. SDS (0.1 g) acted as a stabilizer (Mutia Anissa et al. 2019), silicone oil (few drops) as an anti-foaming agent (Aziz et al. 2019), Wingstay L as an antioxidants (2 phr), and  $N_2H_4$  (0.54 mol) were added. The temperature was maintained at 50 °C and a peristaltic pump was used to add a mixture of boric acid (1.5 g) and 35% aqueous  $H_2O_2$  (1.08 mol) dropwise at a pre-determined addition rate. The obtained HNBR liquid was then filtered using a wire mesh and spread on a glass plate using a casting knife with a thickness between 0.1 and 0.3 mm. Finally, it was dried in the oven at 60 °C for further HNBR latex characterizations.

CALCULATION OF HYDROGENATION DEGREE

According to the American Standard Test procedure (ASTM) D5670-95, calculation of hydrogenation degree was based on the corresponding absorbance in attenuated total reflectance-Fourier transform infrared (ATR-FTIR) at 723, 970, and 2236  $cm^{-1}$ , which corresponded to bending (rocking) vibration of  $sp^2$  C-H, bending (rocking) vibration of  $sp^3$  C-H, and stretching vibration of nitrile groups. The calculation is shown in Scheme 2.

$$\text{Let } A(723) = \frac{A_{723}}{A_{2236}};$$

$$A(970) = \frac{A_{970}}{A_{2236}};$$

$$K(723) = 0.255, \\ \text{which is a constant specific to peak at } 723 \text{ cm}^{-1};$$

$$K(970) = 2.3, \\ \text{which is a constant specific to peak at } 970 \text{ cm}^{-1};$$

$$F = 1 + A\left(\frac{970}{K(970)} + \frac{A(723)}{K(723)}\right);$$

The relative amount of  $C = C$  remaining in HNBR is:

$$C(BR) = \frac{A(970)}{K(970).F};$$

The relative amount of methylene groups formed through hydrogenation:

$$C(HBR) = \frac{A(723)}{K(723).F};$$

Degree of hydrogenation, % =

$$100 - \frac{C(BR)}{C(BR) + C(HBR)} \times 100$$

SCHEME 2. Calculation of hydrogenation degree

where the values of  $A_{723}$  are taken from peak intensity at 723  $cm^{-1}$ ;  $A_{970}$  from peak intensity at 970  $cm^{-1}$ ; and  $A_{2236}$  from peak intensity at 2236  $cm^{-1}$ .

GEL CONTENT ANALYSIS

The ASTM D2765 standard method was used in calculating the gel content percentage. A thin layer of latex between 0.1 and 0.3 mm was spread on a glass plate using a casting knife. The film was then dried in a drying oven at 60 °C for 2 h. After that, the film was peeled off and cut into small pieces. A piece of the sample and methyl ethyl ketone (100 mL) were added into the jar and agitated for 16 h. After 16 h of agitation, the methyl ethyl ketone and the insoluble dried rubber were left to separate them. The amount of insoluble dried rubber present in the methyl ethyl ketone was expressed as gel content. The solution was then filtered using filter paper. The filtered solution (5 mL) was transferred into a shallow foil cup. The shallow foil cup filled with the solution was kept under an infrared lamp for drying. After 2 h, the shallow foil cup was cooled to room temperature before being weighed. The percentage of gel content was calculated in Scheme 3:

$$\text{Weight of dry sample (g)} = A$$

$$\text{Weight of shallow foil cup (g)} = B$$

$$\text{Weight of shallow foil cup + dried contents (g)} = C$$

$$\%TSC \text{ of solvent } \left(\frac{w}{v}\right) = \frac{(C - B) \times 100}{5} = D$$

Total weight of dissolve rubber (in 100 mL solvent) =

$$\frac{(100 \times D)}{100} = E$$

$$\text{Gel content (\%)} = \frac{(1 - E)}{A} \times 100$$

SCHEME 3. Calculation of gel content percentage



The amount of dried rubber that dissolves in the methyl ethyl ketone solvent from the 5 mL filtered solution is denoted as D in percentage unit, while the total weight of dissolved dried rubber from the overall 100 mL solution is denoted as E. The value 1 in the gel content percentage calculation represents the total of non-dissolved dried rubber and dissolved dried rubber, which were subtracted from the total dissolved rubber (E) and divided with the weight of dry rubber sample (A). Hence, the higher the E value, the lower the gel content percentage.

#### OPTIMIZATION OF HYDROGENATION REACTION

An optimization study using RSM with a central composite rotatable design (CCRD) was conducted to minimize gel content during the hydrogenation of NBR. The goal was to achieve the lowest possible percentage of gel content. The primary output of interest was the percentage of gel content, given that excessive gel formation presented a significant challenge during diimide-mediated hydrogenation. The optimization process was focused on three parameters, which are the mole ratio of  $\text{H}_2\text{O}_2:\text{N}_2\text{H}_4$ , TSC of the latex, and reaction time. These parameters had been investigated as the critical factors that greatly affected the gel content percentage of HNBR. The range of CCRD parameters were selected based on previous findings by Lin (2005), Yusof et al. (2018) and Zhou, Bai and Wang (2004), with some modification based on several preliminary experiments. The study was comprised of a total of 17 experimental runs that explored a range of factors, including 1:1 - 5:1 mole ratio (A), 15% - 35% TSC (B), and 6 - 10 h reaction time (C). The experiments were conducted in a randomized sequence, and after the experimental data were gathered, the mathematical-statistical methodology was evaluated by fitting a polynomial function. Ultimately, the optimal values for each variable were identified.

#### CHARACTERIZATION OF HNBR LATEX

The functional groups and chemical bonds in molecules were analyzed using FTIR based on conventional transmission, reflection, and ATR imaging. ATR-FTIR spectrometer (Cary 630 ATR-FTIR in brand Agilent) was used to ascertain the final conversion of double bonds (C=C) to single bonds (C-C) in the hydrogenated rubber latex. The ATR-FTIR data were collected in the range of 4000 to 650  $\text{cm}^{-1}$ . Also, differential scanning calorimeters (DSC) (214 NETZSCH Polyma type) were used to study the thermal property of glass transition temperature by measuring the quantity of heat absorbed and released for HNBR. Meanwhile, the thermal stability and degradation of HNBR were investigated using TGA (TGA/SDTA 851e from Mettler Toledo). The heating rate of TGA instrument for the analysis was 10  $^{\circ}\text{C}/\text{min}$  from 25 to 800  $^{\circ}\text{C}$ .

Aluminum pan was used to hold the samples and nitrogen gas was purged in the system before the analysis. XRD spectrometer (D8 Advance model from Bruker) was used to study the rubber crystallinity and the sample was exposed to a source of  $\text{CuK } \alpha$  radiation ( $\lambda = 0.1539 \text{ nm}$ ), which was shot at the sample at an angle of  $2\theta$  between  $10^{\circ}$  and  $50^{\circ}$  with a scan rate  $3^{\circ}/\text{min}$ .

#### LATEX STABILITY

A chemical stability test was performed to assess the chemical stability of the raw latex against  $\text{Ca}^{2+}$ . For this assay, 0.004 M  $\text{CaCl}_2 \cdot 2\text{H}_2\text{O}$  was prepared. The pH of the  $\text{Ca}^{2+}$  aqueous solution was adjusted to 9.0 using a 5% KOH solution. The solution was mixed with latex (5 mL) for one-minute using a magnetic stirrer and then weighed to the nearest 0.001 g. Next, a wire mesh (50 microns) was snugly fitted into the filtration holders and the mixture was then poured through the wire mesh. The coagulum retained on the wire mesh was washed with deionized water until the filtrate became clear. The wire mesh dried in the oven at 100  $^{\circ}\text{C}$  for 2 h. The final weight of the coagulum retained on the meshes was obtained by the difference in the wire mesh weight.

Sieved latex (60 g) dispersion was used to test the mechanical stability at 1000 rpm in 20 min using the Yasuda Maron mechanical stability tester. The latex was then poured through the wire mesh, and the coagulum retained on the wire mesh was washed with deionized water until the filtrate became clear. The wire mesh was then dried in the oven at 100  $^{\circ}\text{C}$  for 2 h. The chemical and mechanical stability was calculated as shown in Scheme 4:

$$\% \text{ coagulum} = \frac{(\text{dried mesh} - \text{empty mesh})}{\text{weight of sample}} \times 100$$

SCHEME 4. Calculation of chemical and mechanical stability test

#### RESULTS AND DISCUSSION

##### OPTIMIZATION OF HYDROGENATION REACTION

Optimization of parameters was carried out to obtain an ideal HNBR elastomer that had the lowest gel content produced at a faster reaction time with lower amount of  $\text{H}_2\text{O}_2$  used during synthesis. The quadratic polynomial equation of the HNBR elastomer suited the characteristics of the data. List of experiment data from RSM is displayed in Table 1. According to the experiment's results, the following represents the empirical relationship for the HNBR elastomer between the response and the independent variables within the coding unit as per displayed in Scheme 5:

$$\begin{aligned} \text{R\% of HNBR} = & + 34.83 + 11.80A - 19.20B + 0.66C \\ & - 27.08AB + 23.17AC - 24.42BC \\ & + 8.67A^2 + 18.67B^2 + 16.67C^2 \end{aligned}$$

SCHEME 5. Quadratic polynomial equation of the HNBR elastomer

A, B, and C denoted the coded variables for  $\text{H}_2\text{O}_2:\text{N}_2\text{H}_4$  mole ratio, TSC, and time, respectively. The gel content percentage was influenced by the primary linear effects (A, B, and C), quadratic effects ( $A^2$ ,  $B^2$ , and  $C^2$ ), and interaction effects (AB, AC, and BC) where a mole ratio of  $\text{H}_2\text{O}_2$  to  $\text{N}_2\text{H}_4$  and reaction time indicated a synergistic effect, whereas TSC denoted an antagonistic effect. The quadratic model established an excellent correlation, as indicated by its coefficient of determination  $R^2$  of 0.9995. The  $R^2$  values indicated that the independent variables explained 99.95% of the total variation has been observed in the results. The adjusted coefficient of determination ( $R^2_{\text{adj}}$ ) was determined to be 0.9988. The  $R^2_{\text{adj}}$  value closely resembled the  $R^2$  value, indicating that the statistical model was accurate in describing the responses (Shahrul Fizree Idris et al. 2019). Based on the results, the HNBR elastomer gel content response was figured to be a quadratic polynomial, which facilitated a genuine relationship between the response and the parameters chosen.

Table 2 presents the statistical results in the form of an ANOVA for the quadratic equation of the HNBR elastomer's gel content percentage. Shahrul Fizree Idris et al. (2019) stated that the corresponding coefficient term was more significant, when the F value is larger, and the P value is smaller. The F value and the P value of lack-of-fit for the response from the HNBR were 1.60 and 0.2903, respectively. This showed that the value of F for lack-of-fit is bigger than the P value, which indicated that there was a 29.03% chance that the lack-of-fit would occur due to noise. Moreover, the quadratic model was considered well-suited to the experiment as it exhibited regression and a non-significant lack of fit as shown in Table 2. Hence, it was concluded that the response models for the HNBR elastomer accurately represented the experiment.

Through the examination of the 3D response surface plots in Figure 4, the interaction effect of  $\text{H}_2\text{O}_2:\text{N}_2\text{H}_4$  mole ratio, TSC, and reaction time on the response was comprehended. The 3D response surface graphic allowed the determination of the optimal level for each parameter to achieve the desired response. According to the 3D response surface plots, the relation between  $\text{H}_2\text{O}_2:\text{N}_2\text{H}_4$  mole ratio and TSC of rubber yielded the lowest gel content percentage at 32% with 1:1  $\text{H}_2\text{O}_2:\text{N}_2\text{H}_4$  mole ratio, when the TSC of rubber was 25% (Figure 4(a)). The relation between  $\text{H}_2\text{O}_2:\text{N}_2\text{H}_4$  mole ratio and reaction time

yielded the lowest gel content percentage at 32% with 1:1  $\text{H}_2\text{O}_2:\text{N}_2\text{H}_4$  mole ratio and the reaction time was 8 h (Figure 4(b)). Meanwhile, the relation between TSC of rubber and reaction time showed the lowest gel content at 34% with 35% TSC and 8 h reaction time (Figure 4(c)).

The highest gel content was observed at 73%, when the mole ratio of  $\text{H}_2\text{O}_2$  to  $\text{N}_2\text{H}_4$  was 3:1 and the TSC of NBR was 15% during an 8-h reaction period. Furthermore, presence of free radicals in the system could cause a side reaction during the hydrogenation of NBR using diimide, resulted in the formation of heavily gelled products (Yusof et al. 2018). Optimization of  $\text{H}_2\text{O}_2:\text{N}_2\text{H}_4$  mole ratio, TSC of latex and reaction time were conducted to yield a minimum gel content percentage when varying these parameters. Hence, it was deduced by the RSM that the optimum parameter was observed at a mole ratio of 1:1 ( $\text{H}_2\text{O}_2:\text{N}_2\text{H}_4$ ), a TSC of 25%, and a reaction time of 8 h, which yielded 32% gel content.

#### EFFECT OF THE AMOUNT OF HYDROGEN PEROXIDE ON GEL CONTENT

The mole ratio of  $\text{H}_2\text{O}_2:\text{N}_2\text{H}_4$  was varied to investigate the effect of different quantities of  $\text{H}_2\text{O}_2$  utilized.  $\text{H}_2\text{O}_2$  acted as an oxidizing agent for  $\text{N}_2\text{H}_4$  in the system, resulted in the production of diimide. As the mole ratio of  $\text{H}_2\text{O}_2:\text{N}_2\text{H}_4$  was increased from 1:1 to 5:1, the gel content showed an increment as well (Table 3). Zhou, Bai and Wang (2004) also examined the impact of each chemical used on gel production and determined that  $\text{H}_2\text{O}_2$  was the primary factor responsible for crosslinking in HNBR. This happened in all reactions where  $\text{H}_2\text{O}_2$  was present, whether it was reacting with NBR latex by itself or with other chemicals. The dried HNBR formed a large amount of gel. In addition, tests with other reactants, such as  $\text{N}_2\text{H}_4$ , boric acid, or mixes of these chemicals without  $\text{H}_2\text{O}_2$  produced gel content that was about the same as the control NBR latex, which was low.

$\text{H}_2\text{O}_2$  was highly unstable due to the peroxide bond present, and at elevated concentrations of  $\text{H}_2\text{O}_2$ , a cross-linking reaction took place instead (Ngudsuntear, Limtrakul & Arayapranee 2022b; Yusof et al. 2018). This side reaction has led to a reduction in the hydrogenation reaction occurred at the carbon double bond area of the polymer as elucidated in Scheme 6 (De Sarkar, De & Bhowmick 2000). Furthermore, an excessive amount of  $\text{H}_2\text{O}_2$  could lead to the decomposition of  $\text{H}_2\text{O}_2$  and produce hydroxyl radicals that attacked the polymeric chain of the NBR latex, which caused it to either break or become cross-linked, resulting in the gel production (Ngudsuntear, Limtrakul & Arayapranee 2022b; Yusof et al. 2018).

TABLE 1. List of experimental data from RSM

Runs	Factor 1 A: H <sub>2</sub> O <sub>2</sub> :N <sub>2</sub> H <sub>4</sub> mole ratio	Factor 2 B: TSC, %	Factor 3 C: Time, hour	Response 1 Gel content, %
1	1:1	15	6	57
2	5:1	35	6	45
3	1:1	15	10	61
4	1:1	35	10	28
5	5:1	35	10	44
6	1:1	25	8	32
7	5:1	25	8	55
8	3:1	15	8	73
9	3:1	35	8	34
10	3:1	25	6	51
11	3:1	25	10	52
12	3:1	25	8	35
13	3:1	25	8	35
14	3:1	25	8	35
15	3:1	25	8	34
16	3:1	25	8	35
17	3:1	25	8	35

TABLE 2. Statistical ANOVA data from RSM

Source	Sum of squares	Degree of freedom	Mean square	F-value	p-value
Model	2534.75	9	281.64	1442.64	<0.0001
A- H <sub>2</sub> O <sub>2</sub> :N <sub>2</sub> H <sub>4</sub> mole ratio	464.13	1	464.13	2377.27	<0.0001
B- TSC	1228.80	1	1228.80	6293.85	<0.0001
C-Time	2.67	1	2.67	13.66	0.0077
AB	303.52	1	303.52	1554.62	<0.0001
AC	189.42	1	189.42	970.21	<0.0001
BC	210.41	1	210.41	1077.73	<0.0001
A2	112.67	1	112.67	577.07	<0.0001
B2	522.67	1	522.67	2677.07	<0.0001
C2	416.67	1	416.67	2134.15	<0.0001
Residual	1.37	7	0.1952		
Lack of fit	0.5333	2	0.2667	1.60	0.2903
Pure Error	0.8333	5	0.1667		
Corrected Total	2536.12	16			

TABLE 3. Effect of Ratio of H<sub>2</sub>O<sub>2</sub>:N<sub>2</sub>H<sub>4</sub> on gel content

Mole ratio of H <sub>2</sub> O <sub>2</sub> :N <sub>2</sub> H <sub>4</sub>	Gel content, %
1:1	32
3:1	35
5:1	55

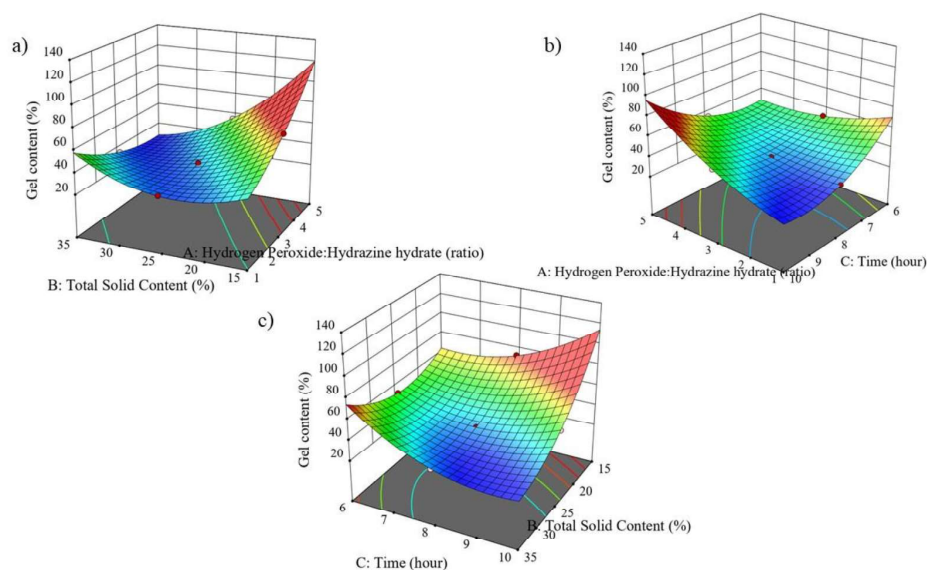
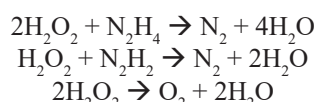


FIGURE 4. 3D surface plots of the parameters (a) the relation between  $\text{H}_2\text{O}_2:\text{N}_2\text{H}_4$  mole ratio and TSC; (b) the relation between reaction time and  $\text{H}_2\text{O}_2:\text{N}_2\text{H}_4$  mole; (c) the relation between TSC and reaction time against response (gel content percentage)



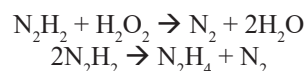
SCHEME 6. Side reaction equations of  $\text{H}_2\text{O}_2$

#### EFFECT OF TOTAL SOLID CONTENT ON GEL CONTENT

Differences in the weight of the rubber after being modified and dried was known as the TSC of the rubber (Herlinawati et al. 2022). Table 4 demonstrates the influence of the overall solid content on the gel content. A decrease in the proportion of TSC led to a rise in gel content. The increased water concentration in the solution, caused by a low percentage of total solid material, improved the process of adding hydrogen to diimide, as described by Ngudsuntear, Limtrakul and Arayaprane (2022). An increased water content reduced the viscosity of the latex, facilitated its blending with other substances and consequently improved the production of diimides for the hydrogenation procedure (Wong, Munusamy & Ong 2019).

Lin (2005) suggested a strong correlation between crosslinking and diimide, as both the homogeneous diimide hydrogenation in organic solvents method and the diimide hydrogenation of unsaturated polymer latex without solvent addition, resulted in the formation of gels. According to Lin (2005), gel formation did not occur when the hydrogenation degree was below 60%. The available evidence suggested that a decrease in the overall solid content enhanced the extent of hydrogenation, which facilitated the addition of hydrogen by diimide and subsequently promoted the

occurrence of side reactions of diimide (Scheme 7). Hence, led to a significant formation of gel.



SCHEME 7. Side reaction equations of diimide

#### EFFECT OF REACTION TIME ON GEL CONTENT

The gel content reached its lowest value within the 8-h reaction (Table 5). With an increase in reaction time from 6 to 8 h, there was a reduction in gel content. This was most likely due to the polymeric chain becoming more saturated and less prone to cross-linking. Moreover, the process of hydrogenation was only possible when the diimide was produced through the redox reaction of  $\text{N}_2\text{H}_4$  and  $\text{H}_2\text{O}_2$  (Shahrul Fizree Idris et al. 2019). This study also show that the 8-h reaction period was the most optimum duration for diimide molecules to diffuse efficiently.

Throughout the hydrogenation process,  $\text{H}_2\text{O}_2$  was added gradually, and the decreased reaction time increased the rate of  $\text{H}_2\text{O}_2$  addition with each drop. This resulted in significant gel formation during the 6-h reaction due to the excessive and frequent addition of  $\text{H}_2\text{O}_2$  into the system. These conditions led to the occurrence of side reactions involving  $\text{H}_2\text{O}_2$  (Scheme 6) and the high formation of gel. Nevertheless, the gel content exhibited a significant rise throughout the 10-h reaction period due to the extremely low rate, at which  $\text{H}_2\text{O}_2$  was added. This slow addition rate facilitated the continuous production of diimide, hence enhanced the



extent of hydrogenation. The persistent generation of diimide led to the side reaction (Scheme 7), and led to the formation of gel due to the high reactivity of diimide reactive substance (De Sarkar, De & Bhowmick 2000; Zhou, Bai & Wang 2004).

CHARACTERIZATION OF HYDROGENATED  
NITRILE BUTADIENE RUBBER

ATTENUATED TOTAL REFLECTANCE  
FOURIER-TRANSFORM INFRARED (ATR-FTIR)

A noticeable peak at 2236  $\text{cm}^{-1}$  in the IR spectrum indicated that the stretching vibration of nitrile groups in the polymer chain remain unchanged during the hydrogenation process. Simultaneously, the intensity of the peak at 970  $\text{cm}^{-1}$ , which corresponds to the bending (rocking) vibration of  $sp^2$  C–H steadily decreased with an increase in hydrogenation degree. New peaks at 723  $\text{cm}^{-1}$  and 1370  $\text{cm}^{-1}$  appeared as a result of the increased bending (rocking) vibration of  $sp^3$  C–H and

bending (scissoring) vibration of  $sp^3$  C–H, respectively, as the hydrogenation degree increases (Liu et al. 2022; Wang et al. 2020). The ATR-FTIR peaks for NBR and HNBR are shown in Table 6. The hydrogenation degree was calculated using the peaks observed at 723, 970, and 2236  $\text{cm}^{-1}$ . Figure 5 displays the infrared spectra of NBR and HNBR latex at different degrees of hydrogenation: 75, 86, 92, and 99%. The different degree of hydrogenation confirms the successful process of hydrogenating NBR.

DIFFERENTIAL SCANNING CALORIMETRY (DSC)

Modification of the chemical composition of the unsaturated component of NBR had occurred, as indicated by an increment in  $T_g$ , which was closely correlated with the extent of hydrogenation. The observed increase in  $T_g$  of the hydrogenated products (Figure 6), could be attributed to the replacement of unsaturated units (C=C), which were the non-crystalline segments in the polymer chain, with ethylene-

TABLE 4. Effect of total solid content on gel content

Total solid content, %	Gel content, %
15	73
25	32
35	34

TABLE 5. Effect of reaction time on gel content

Reaction time, (h)	Gel content, %
6	51
8	32
10	52

TABLE 6. FTIR peak assignation for NBR and HNBR

Wavenumber ( $\text{cm}^{-1}$ )	Peak assignation	Description
2236	-CN	This peak is used as the internal standard for the calculation of degree of hydrogenation
970	=CH- in 1,4-trans unit	This peak decreases in strength and disappears during the hydrogenation
920	=CH- in 1,2 unit	This peak decreases in strength and disappears during the hydrogenation
750	=CH- in 1,4-cis unit	This peak decreases in strength and disappears during the hydrogenation
723	Saturated $-\text{[CH}_2\text{]}_n\text{- unit (n>4)}$ in HNBR	This peak appears and increase in strength during the hydrogenation

propylene units (C-C), which represent the crystalline segments. These studies by Ngudsuntear, Limtrakul and Arayapranee (2022), Petrukhina, Golubeva and Maksimov (2019), and Wang et al. (2020) suggested that the hydrogenation increases crystallinity and presence of crystalline segments in the polymer tended to decrease its mobility, which led to a higher  $T_g$ .

#### THERMOGRAVIMETRIC ANALYSIS (TGA)

The assessment of thermal stability by determining the decomposition temperature using TGA is shown in Figure 7. HNBR has reached a maximum decomposition temperature ranging from 431.4 to 475.1 °C with a hydrogenation degree of 99%. As the degree of hydrogenation elevated, the temperature of the decomposition correspondingly elevated. Table 7 demonstrates that the decomposition temperature of HNBR showed an upward trend as the quantity of C=C bonds decreased. Hydrogenation increases crystallinity, and in crystalline regions, polymer chains have restricted mobility due to their ordered arrangement and higher van der Waals intermolecular force. This restricts the movement of polymer chains, reducing the likelihood of chain scission or other thermal degradation mechanisms. Hence, the overall thermal stability of the polymer increases with a corresponding increase in the decomposition temperature (Liang, Dong & Yue 2019; Liu et al. 2020).

#### X-RAY DIFFRACTION (XRD)

The samples exhibited an amorphous state at ambient temperature, as indicated by the existence of a wide halo centered at  $2\theta = 19^\circ$  (Figure 8). The highly cross-linked latex sample with 99% degree of hydrogenation was the only one that showed a broad peak and a slightly sharp peak in the diffraction profiles, indicated the presence of a low-crystalline region and suggested that the sample had semi-crystalline properties (Li 2020). The broad peaks in both HNBR and NBR observed in XRD analysis were associated with the amorphous regions of the polymer. These amorphous regions were lacking a long-range repeating order of atoms or molecules, which produced broad XRD peaks. It had appeared as a hump or amorphous peak in the XRD pattern. In contrast, the crystalline regions were characterized by a more ordered atomic arrangement, resulting in sharp, well-defined diffraction peaks (Amech 2019).

#### LATEX STABILITY

Chemical and mechanical stability testing aids in determining the tendency of latex particles to agglomerate or form clusters. A latex formulation can be considered stable, when there is a reduced occurrence of coagulation. The chemical stability test evaluates the ability of the latex to resist the presence of  $Ca^{2+}$  ions. This test was used to assess the chemical stability of a NBR latex that was commonly used in the production of

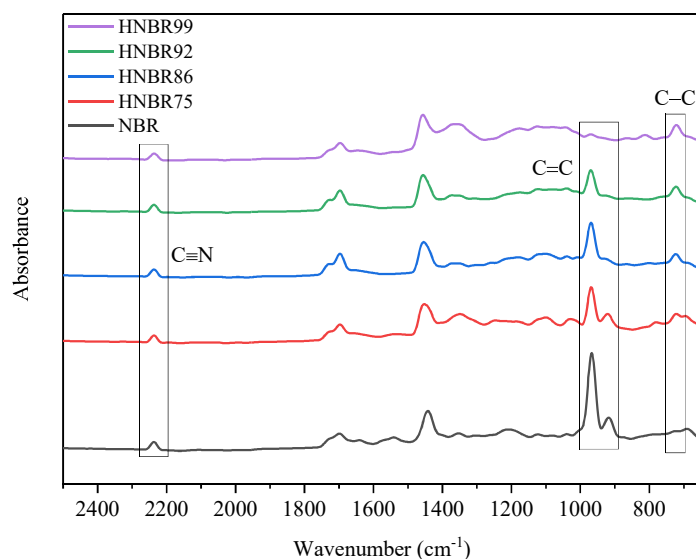


FIGURE 5. ATR-FTIR spectrums of NBR and HNBR

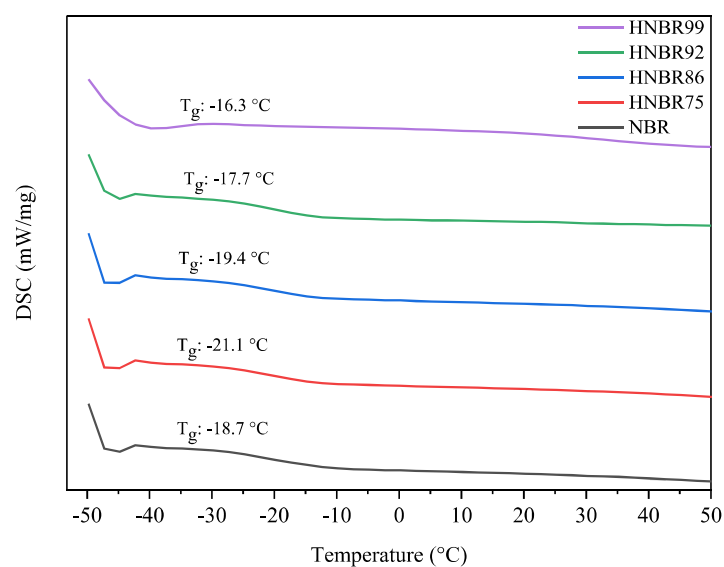


FIGURE 6. DSC thermograms of NBR and HNBR

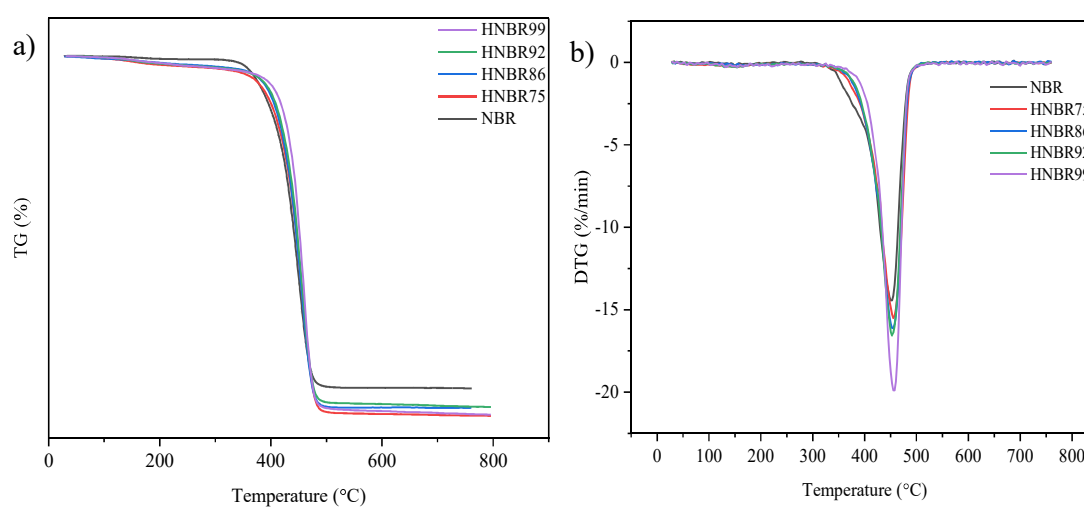


FIGURE 7. TGA thermogram (a) and DTG thermogram (b) of NBR and HNBR

TABLE 7. Decomposition temperature of NBR and HNBR of various degree of hydrogenation

Material	Decomposition temperature, °C
NBR	409.3 - 470.8
HNBR75	418.3 - 476.6
HNBR86	418.6 - 474.7
HNBR92	422.0 - 474.8
HNBR99	431.4 - 475.1

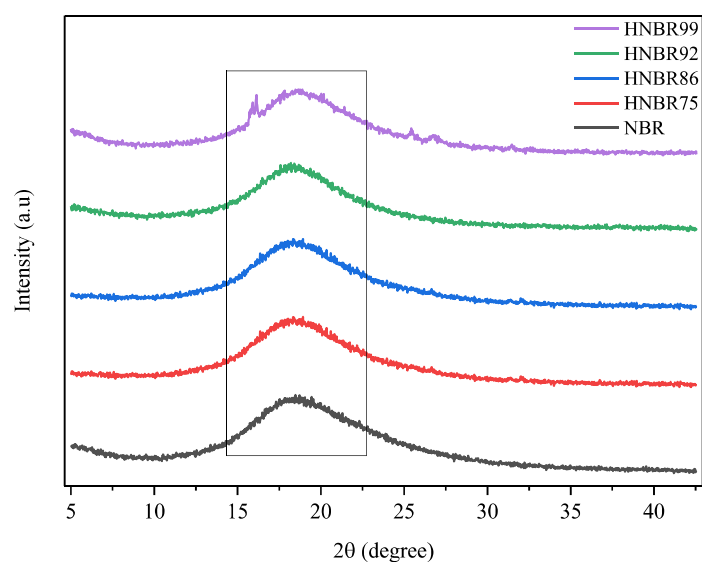


FIGURE 8. XRD pattern of various degree of hydrogenation

TABLE 8. Latex stability test

Material	Chemical stability (Coagulum percentage, %)	Mechanical stability (Coagulum percentage, %)
NBR	0.0016	0.0318
HNBR	0.0003	0.0022

dip-formed articles like gloves, boots, and balloons (Yew et al. 2020). On the other hand, the mechanical stability test evaluates the latex's ability to resist coagulation when subjected to mechanical stress (Mandlekar, Joshi & Butola 2022). The coagulum content percentage of HNBR obtained at 0.0003 and 0.0022 (Table 8), indicated enhanced chemical and mechanical stability of HNBR latex, respectively.

#### CONCLUSION

The utilization of diimide for hydrogenation effectively achieved a simplified procedure that eliminated the requirement for expensive catalysts, hydrogen gas, organic solvents, and the difficulty of catalyst separation in the conventional hydrogenation method. The ideal reaction conditions for achieving a minimal gel content percentage were effectively determined via the utilization of RSM. These conditions comprised a 1:1 mole ratio of  $H_2O_2:N_2H_4$  and a TSC of 25% throughout the duration of an 8-h reaction, which yields 92% hydrogenation degree with 32% gel content. HNBR also exhibited enhanced chemical and mechanical stability, as evidenced by its reduced coagulum content.

#### ACKNOWLEDGEMENTS

The authors acknowledge Synthomer Sdn. Bhd. for the research grant (ST-2022-022) and Centre for Research and Instrumentation (CRIM) at Universiti Kebangsaan Malaysia (UKM) for their research facilities and instrumentation throughout this investigation.

#### REFERENCES

- Ameh, E.S. 2019. A review of basic crystallography and x-ray diffraction applications. *The International Journal of Advanced Manufacturing Technology* 105(7): 3289-3302.
- Aziz, T., Fan, H., Khan, F.U., Haroon, M. & Cheng, L. 2019. Modified silicone oil types, mechanical properties and applications. *Polymer Bulletin* 76(4): 2129-2145.
- De Sarkar, M., De, P.P. & Bhowmick, A.K. 2000. Diimide reduction of carboxylated styrene – butadiene rubber in latex stage. *Polymer* 41(3): 907-915.
- Herlinawati, E., Montoro, P., Ismawanto, S., Syafaah, A., Aji, M., Giner, M., Flori, A., Gohet, E. & Oktavia, F. 2022. Dynamic analysis of tapping panel dryness in *Hevea brasiliensis* reveals new insights on this physiological syndrome affecting latex production. *Heliyon* 8(10): 10920.

- Li, C.Y. 2020. The rise of semicrystalline polymers and why are they still interesting. *Polymer* 211: 123150.
- Liang, L., Dong, J. & Yue, D. 2019. Branched EHNBR and its properties with enhanced low-temperature performance and oil resistance. *RSC Advances* 9(55): 32130-32136.
- Lin, X. 2005. Hydrogenation of unsaturated polymers in latex form. Ph.D. Thesis, University of Waterloo, Ontario, Canada (Unpublished).
- Liu, X., Fu, Y., Zhou, D., Chen, H., Li, Y., Song, J., Zhang, S. & Wang, H. 2022. Hydrogenation of carboxyl nitrile butadiene rubber latex using a ruthenium-based catalyst. *Catalysts* 12(1): 97.
- Liu, J., Sun, J., Zhang, Z., Yang, H. & Nie, X. 2020. One-step synthesis of end-functionalized hydrogenated nitrile-butadiene rubber by combining the functional metathesis with hydrogenation. *ChemistryOpen* 9(3): 374-380.
- Luo, Z.H., Feng, M., Lu, H., Kong, X.X. & Cao, G.P. 2019. Nitrile butadiene rubber hydrogenation over a monolithic Pd/CNTs@Nickel foam catalysts: Tunable CNTs morphology effect on catalytic performance. *Industrial and Engineering Chemistry Research* 58(5): 1812-1822.
- Mandlekar, N., Joshi, M. & Butola, B.S. 2022. A review on specialty elastomers based potential inflatable structures and applications. *Advanced Industrial and Engineering Polymer Research* 5(1): 33-45.
- Mutia Anissa Marsya, Bismo Dwi Putranto, Santi Puspitasari, Adi Cifriadi & Mochamad Chalid 2019. Catalyst screening on diimide transfer hydrogenation of natural rubber latex catalyst screening on diimide transfer hydrogenation of natural rubber latex. *IOP Conference Series: Materials Science and Engineering* 509: 012078.
- Ngudsuntear, K., Limtrakul, S. & Arayaprane, W. 2022. Synthesis of hydrogenated natural rubber having epoxide groups using diimide. *ACS Omega* 7(25): 21483-21491.
- Nguyen Duy, H., Rimdusit, N., Tran Quang, T., Phan Minh, Q., Vu Trung, N., Nguyen, T.N., Nguyen, T.H., Rimdusit, S., Ougizawa, T. & Tran Thi, T. 2021. Improvement of thermal properties of Vietnam deproteinized natural rubber via graft copolymerization with styrene/acrylonitrile and diimide transfer hydrogenation. *Polymers for Advanced Technologies* 32(2): 736-747.
- Petrukhina, N.N., Golubeva, M.A. & Maksimov, A.L. 2019. Synthesis and use of hydrogenated polymers. *Russian Journal of Applied Chemistry* 92(6): 715-733.
- Puspitasari, S., Falaah, A.F. & Zanki, A.N. 2019. Selection of stabilizer and coagulant for natural rubber latex colloidal system during diimide catalytic hydrogenation at semi pilot scale reaction Selection of stabilizer and coagulant for natural rubber latex colloidal system during diimide catalytic hy. *IOP Conference Series: Materials Science and Engineering* 509: 012128.
- Shahrul Fizree Idris, M., Hanis Adila Azhar, N., Firdaus, F., Efliza Ashari, S. & Fairus Mohd Yusoff, S. 2019. Effect of temperature, time and diimide/rubber ratio on the hydrogenation of liquid natural rubber by response surface methodology. *Indonesian Journal of Chemistry* 19(4): 882-891.
- Wang, X., Sun, J., Xia, L., Wang, C., Kim, J.K. & Zong, C. 2020. Kinetics of hydrogenation of acrylonitrile butadiene rubber: A latex-based *in situ* and low-temperature approach. *Colloid and Polymer Science* 298(11): 1501-1513.
- Wong, J.L.O., Munusamy, Y. & Ong, K.S. 2019. Effect of total solids content of nitrile rubber latex on coating performance of phase change material. *AIP Conference Proceedings* 2157: 020046.
- Yew, G.Y., Tham, T.C., Show, P.L., Ho, Y.C., Ong, S.K., Law, C.L., Song, C. & Chang, J.S. 2020. Unlocking the secret of bio-additive components in rubber compounding in processing quality nitrile glove. *Applied Biochemistry and Biotechnology* 191: 1-28.
- Yusof, M.J.M., Tahir, N.A.M., Firdaus, F. & Yusoff, S.F.M. 2018. Diimide reduction of liquid natural rubber in hydrazine hydrate/hydrogen peroxide system: A side reaction study. *Malaysian Journal of Analytical Sciences* 22(6): 1023-1030.
- Zhang, J., Wang, C., Zao, W., Feng, H., Hou, Y. & Huo, A. 2020. High-performance nitrile butadiene rubber composites with good mechanical properties, tunable elasticity, and robust shape memory behaviors. *Industrial and Engineering Chemistry Research* 59(36): 15936-15947.
- Zhou, S., Bai, H. & Wang, J. 2004. Hydrogenation of acrylonitrile - butadiene rubber latexes. *Journal of Applied Polymer Science* 91(4): 2072-2078.

\*Corresponding author; email: sitifairus@ukm.edu.my